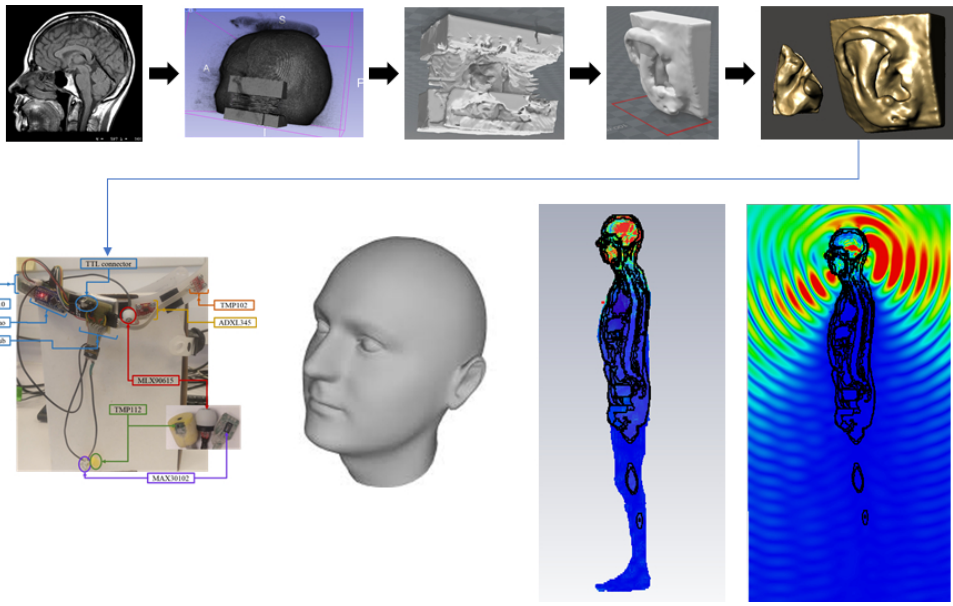


**Multimodal minimally invasive wearable technology for
epilepsy monitoring: a feasibility study of the periauricular
area**

Journal:	<i>IEEE Sensors Journal</i>
Manuscript ID	Draft
Manuscript Type:	Regular Paper
Date Submitted by the Author:	n/a
Complete List of Authors:	Besné, Guillermo M.; Centro de Investigación Médica Aplicada, Biomedical Engineering Program Lopez-Iturri, Peio; EEC Department; Institute of Smart Cities (ISC) Alegre, Manuel; Clínica Universidad de Navarra; Centro de Investigación Médica Aplicada, Biomedical Engineering Program Artieda, Julio; CIMA (Universidad de Navarra) Trigo, Jesus Daniel; Universidad Publica de Navarra, Electrical, Electronic and Communications Engineering; Institute of Smart Cities (ISC) Serrano, Luis; Public University of Navarra, EEC Department; Institute of Smart Cities (ISC) Falcone, Francisco; UPNA, EEC Department; Institute of Smart Cities (ISC); Tecnológico de Monterrey, School of Engineering and Sciences Valencia, Miguel; Centro de Investigación Médica Aplicada, Biomedical Engineering Program
Keywords:	APPL

1
2
3
4
5
6
7
8
9
10
11
12
13
14
15
16
17
18
19
20
21
22
23
24
25
26
27
28
29
30
31
32
33
34
35
36
37
38
39
40
41
42
43
44
45
46
47
48
49
50
51
52
53
54
55
56
57
58
59
60



600x358mm (38 x 38 DPI)

Multimodal minimally invasive wearable technology for epilepsy monitoring: a feasibility study of the periauricular area

Guillermo M. Besné, Peio Lopez-Iturri, Manuel Alegre, Julio Artieda, Jesús D. Trigo, Luis Serrano-Arriezu, Francisco Falcone, *Senior Member, IEEE* and Miguel Valencia

Abstract—Ambulatory monitoring is of great interest in both clinical and domestic environments. Despite of the technological advances, few monitoring solutions are suitable for medical application and diagnosis. Here we investigate the feasibility of targeting the peri-auricular area (ear pavilion, ear canal and the surrounding skin areas) to implement a multimodal system that fulfills the requirements of ergonomics and minimal obstructiveness in the context of epilepsy monitoring. Six physiological signals are selected and explored for their integration in the area of interest and a “proof of concept” prototype integrating the components in a single portable device targeting the selected location is implemented. Results show mixed results where some parameters are highly reliable, and others are impractical or require customized technology to provide clinically relevant information. To enable data acquisition, storage and processing within Internet of Medical Things paradigms, wireless body area transceiver integration is also analyzed in terms of coverage/capacity relations, showing feasibility for such device configuration.

Index Terms—Ambulatory monitoring, Multimodal Wearable, Periauricular area, Epilepsy

I. Introduction

THE chronification of some diseases and the increase in technological knowledge by the general population results on a higher number of medical experts, patients and relatives demanding a better use of technological innovations. Their claim: to ensure accurate diagnosis, provide continuous monitoring and personalized treatments [1-5].

In recent years, technological advances have made it possible to implement increasingly versatile sensors, smaller in size and with lower consumption. These developments, together with the possibility of transmitting, processing, and storing a large amount of information might represent a shift of paradigm in the way we understand and use “data” for disease management. Technology has improved consumer electronics leading to a surge of wearable devices capable of

This project was supported in part by the Department of Economic Development of the Government of Navarra, (ref. GN 2019 PC078-079) and the Carlos III Health Institute through the project “DTS19 / 00130”. (Co-financed by the European Regional Development Fund; “A way to make Europe”). Guillermo Besné acknowledges the “Asociación de Amigos de la Universidad de Navarra, ADA” for the economic support during his PhD.

G. M. Besné, M. Alegre, J. Artieda and M. Valencia are with the Biomedical Engineering Program, CIMA, Universidad de Navarra, 31080 Pamplona, Spain, and with the IdiSNA, Instituto de Investigación Sanitaria de Navarra, 31008 Pamplona, Spain (e-mail: mvustarroz@unav.es).

P. Lopez-Iturri, J.D. Trigo, L. Serrano-Arriezu and F. Falcone are with the Institute of Smart Cities, Public University of Navarre, 31006 Pamplona, and the IdiSNA, Instituto de Investigación Sanitaria de Navarra, 31008 Pamplona, Spain (e-mail: francisco.falcone@unavarra.es).

F. Falcone is also with the School of Engineering and Sciences, Tecnológico de Monterrey, Monterrey 64849, Mexico

M. Alegre is also with Clínica Universidad de Navarra (CUN), 31008 Pamplona, Spain.

monitoring physiological parameters such as heart rate, calories consumption, physical exercise intensity or estimates of sleep stages. However, very few of these solutions are suitable for medical application and diagnosis [6]. This might be explained by the fact that the process of adopting some technological solution for monitoring diseases is not easy. [7-10]. Leaving aside concepts such as privacy and clinical data security, their success lies in the ability to implement features such as i) portability, ii) ease of use, iii) robustness iv) precision (as compared to those provided by clinical and specialized settings) and v) coverage of parameters to provide (clinically) relevant information. In addition, and depending on the disease or monitoring circumstances, it is necessary to identify -among others-, the most suitable variables of interest, location/optimization of the sensitization points, degree of miniaturization, level of obstruction, anatomic constraints, or ergonomics needs.

Continuous monitoring and personalized follow-up is of high interest in diseases such as epilepsy: a chronic neurologic condition marked by the recurrence of unprovoked seizures [11,12]. Seizures are paroxysmal events that result from abnormal neuronal discharges and manifest in the form of sudden, stereotyped episodes with accompanying changes in motor activity, sensation, and behavior, thus exposing the patient to life-threatening situations [13,14]. Seizures result in increased injuries and mortality, including sudden unexpected death in epilepsy (SUDEP). This scenario makes constant supervision a requirement, even during night [15,16]. The need of chronic intake of antiepileptic drugs (AEDs) lead also to potential side effects that require continuous adjustment of the treatment. Despite of handwritten diaries where patients’ evolution is reflected, disease perception and patients’ mood have drastic effects on reports to neurologist and neuro-

1 pediatricians. Consequently, unnecessary or even inadequate
2 treatment adjustments are frequent [17].

3 All these scenarios justify the need for monitoring systems
4 suitable for their operation on domestic or ambulatory
5 environments. Ideally, such developments should implement
6 multimodal, minimally obstructive monitoring systems
7 capable to provide information clinically relevant to assess the
8 physiological and neurological state of the subject. As critical
9 as the parameters to measure, it is also important to identify an
10 appropriate recording location. All parameters selected must
11 be susceptible to be measured, with little or non-intrusive
12 approximation, complying with structural stability capable of
13 supporting robust and prolonged monitoring periods of time.
14 The periauricular area (the external ear, the ear canal and the
15 surrounding skin area) seems to be a good candidate; the
16 anatomical location and rigidity of the ear canal provides great
17 support to anchor potential devices such as earphones or
18 hearing aids with low stigmatization. In addition, previous
19 reports have described the possibility of obtaining reliable,
20 long term and clinically relevant measures of different
21 biosignals. Nevertheless, combining several signal modalities
22 in one single setup represents a big challenge and requires the
23 systematic assessment of their feasibility when being recorded
24 at the same time.

25 In the case of epilepsy patients, a number of such
26 physiological measurements can be of special relevance;
27 parameters such as electroencephalogram (EEG), acceleration
28 (Acc), electrocardiogram (ECG), peripheral oximetry (SpO₂),
29 body core temperature (T^a) and galvanic skin response (GSR)
30 could provide an integral assessment of the general state of the
31 patient.

32 The EEG is the register of electrical activity generated by
33 the brain [18,19]. In the case of epilepsy, the EEG represents
34 one of the most important tools for diagnosis and follow-up. In
35 epileptic patients both, during seizures and interictal periods,
36 the brain generates abnormal activities easily identified in the
37 EEG traces whereas during. In this context, EEG recordings in
38 the ear canal has been introduced recently [20] resulting on
39 different implementations that also include wireless
40 capabilities [21-25]. In the area of interest, the EEG can be
41 recorded through electrodes located within the ear canal (in-
42 earEEG) or disposed around the ear pavilion and provide
43 relevant information for the detection of seizures in patients
44 with focal and generalized epilepsies [26,27].

45 Acceleration represents a straightforward method to
46 quantify the amount of movement. Measurements can refer to
47 dynamic acceleration, where speed changes of the monitored
48 object are quantified; or static acceleration, with
49 measurements are due to gravity, thus making it possible to
50 estimate the objects orientation relative to Earth's surface. In
51 the case of epilepsy, acceleration has been successfully
52 integrated into warning systems to detect seizures [28,29]. In
53 addition, it can be used for fall detection, head orientation
54 assessment [30], to quantify the amount of movement, identify
55 postural changes, or the presence of abnormal movements
56 [31]. As for placement, acceleration measurement of the head
57 is less restrictive with its placement. As a rigid body,
58 movement of the head can be monitored on any point,
59 including the periauricular area.

60 ECG records electrical activity from the heart myocardium

[32]. Polarization and depolarization sequences leading to
heart contraction result in a series of waveforms that can be
divided on P-wave, QRS complex and T-wave. To obtain a
high-quality ECG suitable for cardiovascular diagnosis a set of
9 electrodes are required [33]. However, for simpler
approaches, such as those aimed at estimating the heart rate
(HR) or their variations in time (heartrate variability, HRV),
three or even two electrodes are sufficient. Variations on the
HR are used as surrogates of distress at multiple levels; in the
context of epilepsy they have proved to be useful to detect
occurrence and onset of epileptic seizures [34-36], and
SUDEP events. Nevertheless, and in the case of periauricular
area (under the constraint of unique and unilateral placement
of the electrodes), the geometry of the heart vs (one) ear, could
present some difficulties to provide reliable ECG
measurements.

Photoplethysmography (PPG) measures volumetric
variations of blood circulation through optical inexpensive
methods. By using different light sources and photodetectors
at the surface of skin PPG allows to estimate HR, oxygen
saturation in peripheral blood (SpO₂) and other parameters
suitable for assessing the state of the cardiovascular system
[37,38]. Green light (530nm) sources are optimal to determine
the HR on continuous monitoring setups as it is more sensible
to small volume changes and results more robust against
movement artifacts [39]. Complementary, red (650nm) and
infrared (IR, 940nm) sources are used to exploit absorption
differences of hemoglobin on its reduced (Hb) and oxygenized
(HbO₂) state and permit to extract SpO₂ [40]. In the context
of epilepsy, PPG can serve to estimate HR and HRV as an
alternative to ECG measures. It allows to study
cardiorespiratory coupling changes and SpO₂ levels can be
useful to predict/detect epileptic seizures, although it might be
problematic to implement for tonic-clonic seizures [41-43].
Common placements for PPG sensors include the earlobe, that
it is highly irrigated. Fingers are the most usual, but other
implementations with custom PPG sensors on in-ear devices
have been build and performed satisfactorily acquiring the
PPG signal on the concha or in the ear canal [44].

As endothermic animal, humans can generate regulate their
own body temperature by means of metabolic rate, sweating,
vasoconstriction and other physiological mechanism. The
most common alteration in temperature is fever, an abnormal
rise on core body temperature. The ability of thermoregulation
and being able to withstand external temperature varies at
different ages. Adults have larger bodies and greater volume
to surface ratio, therefore a higher resistance to external
temperatures affecting their core body temperature. As such,
children are more susceptible of suffering hyper- and
hypothermia under the same circumstances [45]. Given this
condition, febrile seizures are more common among children,
making body temperature a critical parameter. This
measurement is even more critical among for some specific
epileptic patients, as they are far more sensitive to temperature
changes and frequently trigger seizures [46]. Measuring core
body temperature –more reliable than peripheral temperature-,
requires placing sensors in specific locations [47]. The
tympanum is one of the best areas to estimate the core
temperature along with the anus or the armpit. Nevertheless,
its applicability is far more convenient and suitable for a

1 sustained monitoring.

2 Galvanic skin response (GSR), also known as electro
3 dermal activity (EDA), measures the conductance or
4 resistance of the skin. GSA is directly related to sweat glands
5 activity that is regulated by sympathetic and parasympathetic
6 nervous systems [48,49]. Arousal of emotional, sensorial or
7 physiological origin modulates the balance between these two
8 systems and modify skin conductance [50]. Application for
9 epilepsy patients include stress levels assessment that could
10 serve to prevent the onset of certain types of seizures; paired
11 with accelerometers, is used to detect convulsive seizures [51]
12 and SUDEP [52]. Previous works performed GSR
13 measurements on multiple areas to confirm their validity [53].
14 Among them, the closest one to the desired area is the neck:
15 placing the electrodes on the nape on both sides of the spine.
16 These works combined with the population of sweat glands on
17 both areas could allow GSR acquisition on this area [54].

18 Here we explore the feasibility of integration of these six
19 selected measures in the periauricular area. Several efforts
20 have succeeded in implementing unimodal devices providing a
21 unique physiological modality of recording. Others have
22 proposed the combination of multiple devices to increase the
23 number of parameters measured, but at the cost of increasing
24 complexity (using several recording points across the body)
25 and decreasing ergonomics and ease of use. Integrating all
26 these measurements in a single device, opens the possibility to
27 implement a multimodal monitoring system, minimally
28 obstructive, and ergonomic, with the capability to gather
29 information that could be crucial in the diagnosis and follow-
30 up of patients, including the capability of providing a SUDEP
31 and seizure warning system, but attending to principles of
32 ergonomics, robustness, and reliability.

33 Finally, and to enable the inclusion of the monitoring
34 platform within medical health systems following the
35 paradigms of Smart Health and the Internet of Medical Things
36 (IoMT), integration of communication system appears as a
37 key factor in the development of such multimodal monitoring
38 system. The proposed approach, taking advantage of wearable
39 devices, requires user mobility as well to provide high
40 ergonomic levels, leading to the use of wireless
41 communication technologies. Among these, body area
42 network (BAN) protocols are widely employed, owing to low
43 form factor, low energy consumption, moderate cost and
44 transmission rates in the 1-2 Mbps range. In this sense,
45 Bluetooth is commonplace in wearable connectivity, tethering
46 either to other wearable devices such as a smart watch,
47 smartphones or to infrastructure gateways, enabling user
48 interaction as well as web/cloud connectivity inherently [63].
49 The integration of wireless transceivers within the sensor
50 platform is conditioned by the characteristics of radio
51 propagation in body area network scenarios, which can
52 consider on-body, off-body and in-body communication links.
53 These specific communication links exhibit losses and
54 potential degradation owing to different effects such as body
55 impact (in terms of penetration losses, shadowing, and
56 scattering), human body dynamics, modification of antenna
57 operational characteristics (e.g., operation frequency,
58 bandwidth, input impedance, radiation diagram) and multipath
59 propagation components from the surrounding environment
60 [64]. Coverage/capacity requirements must be fulfilled to

provide adequate quality of service metrics, in terms of bit
error, rate/block error and rate/latency thresholds. Small scale
statistics as well as path loss approximations have been
obtained to provide assessment in relation with operational
conditions of wireless transceivers operating in body area
network configurations [63,64].

II. MATERIALS AND METHODS

The feasibility and validity of recording the proposed
parameters on the auricular area was performed by first
recording each modality individually and finally integrating all
of them in a former multimodal recording were a proof-of-
principle multimodal system is built. Recordings were
performed in 10 volunteers. Recording equipment, protocols
and paradigms were approved by the local ethical committee
of the University of Navarra (Ref: CEIC-2021.143) following
international guidelines. Inclusion criteria for recruited
subjects were a) age ranging from 20 to 40 years old and b) no
known cardiac, or c) neurological disease.

A. Electroencephalography

Feasibility and validity of recording EEG activity in the
area of interest was performed according to three different
paradigms previously explored [55]. Two electrodes were
placed in periauricular area (above the ear: EarSup and below
the ear: EarInf). As a gold standard, the activity of a third
electrode on the occipital region (Oz position following the
10:20 system) was also recorded. All the three electrodes were
referred to the earlobe and the ground electrode was placed on
the mastoid. EEG recordings were performed by using
BrainAmp EEG amplifiers (BrainProducts,
<https://brainvision.com/>) connected with a STIM2 system
(Compumedics Neuroscan,
<https://compumedicsneuroscan.com/product/stim2-precise-stimulus-presentation/>) to deliver visual stimuli.

Under the α -band modulation paradigm volunteers were
placed on a relaxed position, wake while keeping the eyes
open for 30 seconds. Afterwards, they closed their eyes
(without falling asleep) for another 30 seconds. This was
repeated at least 10 several times, modulating brain's waves
and an increase in the brain activity on the α band (8-12Hz) is
observed. This modulation is compared between recording
areas by performing a power spectrum density (PSD) [56],
[57] for each state, and then quantifying the modulation on the
 α -band and the exact frequency of the peak.

Then we recorded Visual Evoked Potentials (VEP): on a
relaxed position, volunteers were stimulated visually by means
of an alternating chessboard pattern that changed every
1.1667s (~ 0.854 Hz). The alternating patten stimulates the
visual system and elicits prototypic brain responses locked to
the stimulus that show a series of positive and negative peaks
at very specific latencies [58]. Accordingly, we determined the
feasibility of obtaining such responses on the selected area and
compared their latencies with those recorded over the occipital
area.

Finally, we evaluated the Visual Steady-State Responses
(VSSR) on the periauricular region. To do that, we used the
same chessboard stimulus but increasing the frequency to
8.54Hz. Responses were obtained by performing a PSD for

each area and comparing the power and frequency of the main response.

B. Acceleration

Acceleration measurements were performed with the tri-axial linear accelerometer ADXL345 (Analog Devices, <https://www.analog.com/en/products/adxl345.html>). During the recordings, the accelerometer was firmly attached to the side of the head close to the ear and volunteers perform three different sets of movements: postural changes (roll, pitch and yaw) walking and jumping.

To minimize potential effects of the inter-individual differences both in the orientation of the sensor and in the dynamics of the performed activities (e.g. velocities in the execution of the jumping phase), a rotation on the XYZ axis of accelerometer followed by a Dynamic Time Warping (DTW) [59,60] of the signals were computed. By doing so, we were able to align the different time series across paradigms and subjects.

C. Cardiovascular Monitoring

For this experiment two modalities are: electrocardiography (ECG) and photoplethysmography (PPG). In our experiments we used a BiosignalsPlux Explorer system from Plux Biosignals (<https://plux.info/34-kits>); an Arduino-based fully integrated system for physiological research. We evaluated several configurations: a) chest ECG as gold standard (following Plux indications), b) ear ECG, c) PPG on the fingertip as gold standard and d) PPG on the ear canal. To place the PPG sensor on the ear canal and generate some pressure against the tissue, the PPG sensor was embedded in a viscoelastic earplug.

From the ECG, we detected heartbeats and estimated the heart rate (HR). Then, Bland-Altman [61] analysis was used to compare the HR estimated from the chest ECG with those obtained from the ear-ECG, finger PPG and ear PPG.

Next, we explored the possibility to integrate the MAX30102 PPG sensor (<https://www.maximintegrated.com/en/products/interface/sensor-interface/MAX30102.html>) which provides capabilities to provide SpO2 information. Recordings were performed on the following locations: two gold standard areas: fingertip and ear lobe; and two alternative areas: the ear canal and behind the ear (over the mastoid process).

D. Body Temperature

For body temperature assessment, the MLX90615 IR temperature sensor (<https://www.melexis.com/en/product/MLX90615>) and the TMP112 thermocouple (<https://www.ti.com/product/TMP112>) were explored. The MLX90615 is a low power consumption IR temperature sensor with 0.5°C of precision and 0.02°C of resolution. Despite of its small dimensions, it could result problematic for our aim, as it would obstruct completely the ear canal, preventing any aeration and obstructing sound from reaching to the tympanum. The TMP112 is a miniaturized thermocouple-based sensor (1.6x1.6mm), with low consumption, 0.5°C accuracy and 0.0625°C resolution. Complementarily, we also explored the possibility to use the temperature sensor integrated in the MAX30102 PPG (used to

internally calibrate the IR readings of the PPG photodiode). Nevertheless, and although the MAX30102 would be the best choice in terms of potential integration, it has the lowest precision (1°C).

To assess the suitability of these sensors for future implementations we obtained their calibration curves. To do that, sensors were faced to a hot body and the temperature was measured as the temperature drops gradually; a commercial IR thermometer ThermoBaby was used as reference. Then we evaluated the capability of the sensors to follow changes in the temperature; sensors went through three temperature stages: 1) room temperature (around 20°C) for 30 minutes, 2) cold room (around 2°C) for 60 minutes and 3) room temperature for another 30 minutes.

From these analyses we selected the TMP102 thermocouple and proceed with recording on the volunteers. The TMP102 was embedded in a viscoelastic earplug, inserted in the ear canal and subjects were asked to move across several rooms with different temperatures: 2 minutes in an office (room temperature ~20°C), 2 minutes in a ~5°C refrigerated room, 1 minute in a ~-15°C refrigerated room, again back for 2 minutes at the ~5°C room and finally 2 minutes in the office. The exact room temperature was recorded simultaneously with another TMP102 thermocouple.

E. Galvanic Skin Response

The equipment used for GSR validation was again the BiosignalsPlux Explorer with the EDA (electrodermal activity, equivalent to GSR) sensor. To modulate their autonomic response, volunteers were asked to watch 6-minute-long recompilation of short suspense videos and then asked to perform 6 consecutive Valsalva maneuvers. GSR sensors are placed between a) index and middle finger as gold standard and b) the tragus and the mastoid process ipsilaterally to the previous configuration. After visual inspection of the recorded data, analysis on the influence of the maneuvers was determined on frequency bands: 0.1-0.2 Hz, 0.2-0.3 Hz, 0.3-0.4 Hz and 0.4-1.0 Hz [62].

F. Proof of Concept Prototype

Finally, and with a selection of the most suitable components, we proceeded with their integration in a prototype considering factors of a) modularity, b) wearability, c) reliability and d) ease of use. This prototype is designed as a “proof of concept” to test the possibility of performing a simultaneous multimodal recoding of the selected variables together with the ability of a simple microcontroller, such as an Arduino Nano, to manage the components and broadcast the recorded signals through wireless technology. Although in terms of miniaturization, placement and degree of integration the microcontroller specifications were not considered key in this stage of the development, attention was focused on the dimensions and placement of the sensors, that were considered critical to fulfill with the volumetric restrictions imposed by the area of interest (they must be small enough to fit inside or around the ear canal of volunteers).

G. Body Area Network Wireless Connectivity

Different body area network topologies have been considered, employing Bluetooth Classic and Bluetooth Low

Energy (BLE) systems following the path loss methodology described in [64], which considers receiver position at chest or hip and transmitter positions at chest, back, right wrist and left wrist. Different transceiver operation conditions have been considered, in terms of parameters such as use of frequency hopping, transmission power setting or receiver sensitivity thresholds. Further insight is obtained by performing full wave electromagnetic analysis of wireless intrabody propagation links. These results will be further discussed in the following section.

III. RESULTS

In this section, results of the feasibility studies for each individual modality is exemplified by showing the data from a representative subject. Then, a quantitative analysis including all 10 subjects is presented. For the proof of concept prototype, an implementation example with a representative recording is provided. Finally, wireless connectivity modelling results for a BAN are shown.

A. Electroencephalography

Fig. 1 shows the effect of closing the eyes on the modulation of the alpha oscillations for the Oz, EarSup and EarInf locations. Although the amplitude over Oz is larger than that recorded in the ear areas, the analysis of the prominence of the peaks confirms the existence of a significant modulation of the amplitude (but not the frequency) of the alpha rhythm all over the three locations (Fig. 2).

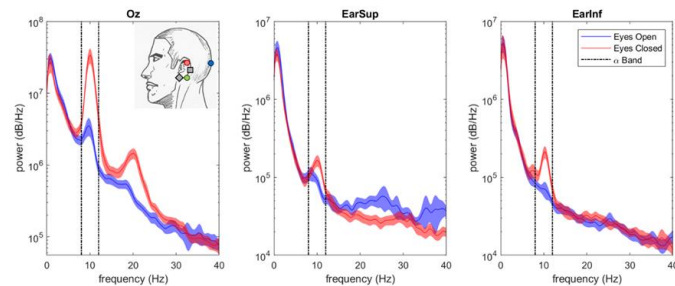


Fig. 1. Power spectrum of the acquired signal during the α -attenuation study of a single subject representing in red the eyes-closed period and in blue the eyes-open period on the corresponding areas: occipital, below the ear and above the ear (left to right).

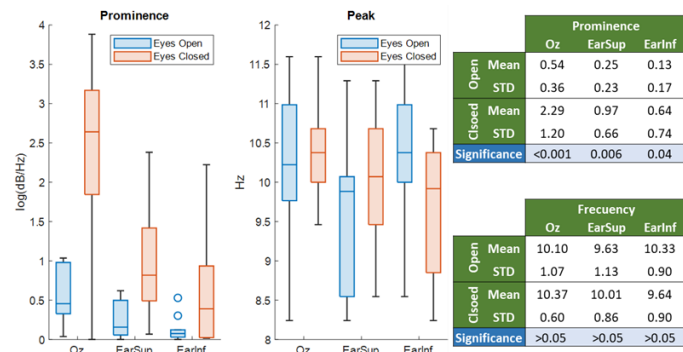


Fig. 2. Study of prominence and frequency of the alpha rhythm modulation during the closed-open eyes study.

For the VEPs, results confirm that the maximal response is detected at Oz; nevertheless, latencies for the N75, P100 and N140 are maintained across the three locations, showing no

significant differences and thus demonstrating that despite of the lower amplitude of the responses, it is possible to obtain VEP responses in the periauricular area (Fig. 3).

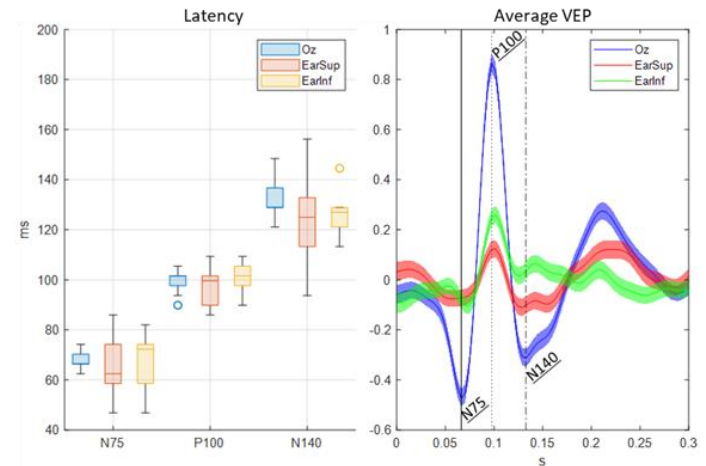


Fig. 3. VEP study representing the delays on N75, P100 and N140 for each electrode (left) and the average VEP for all volunteers at each recording area (right).

As for the case of the VEPs, the VSSR were also detected on the three selected recording areas. Fig. 4 shows the VSSR response from a representative subject together with the analysis of the amplitude and frequency of the responses for the 10 subjects. Results show that although maximal responses are detected at Oz, it is possible to record VSSR in the periauricular area with a good SNR for their detection and with no deviation of the frequency (that is expected to be 8.54Hz).

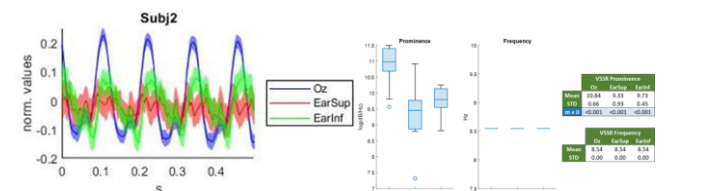


Fig. 4. VSSR of a representative subject at the three selected locations together with the analyses of the prominence and frequency of such responses for the 10 volunteers involved in the study.

B. Acceleration

Fig. 5 shows a 3D representation of the linear acceleration recorded for all subjects. After a coordinate axis rotation (see methods), trajectories show a good concordance between subjects and differences between the three different movements tested (postural changes, walking and jumping). Indeed, a simple correlation analysis (Fig. 6) suggests the suitability of these measures to implement a detection algorithm to identify them. Finally, it is worth to note that the information provided by the static acceleration also allows differentiating between postures within the postural changes test.

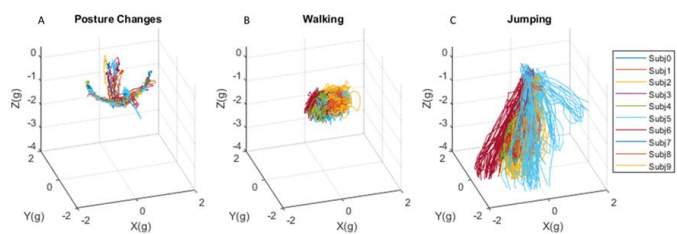


Fig. 5. Tri-axial linear acceleration measurements for the 10 volunteers under a) postural changes, b) walking and c) jumping.

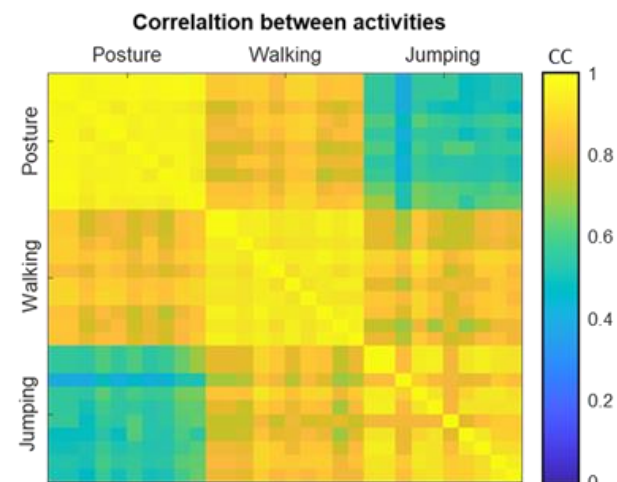


Fig. 6. Correlation values obtained for all recorded activities organized by subject and volunteer.

C. Cardiovascular Monitoring

Fig. 7 shows ECG recordings together with the detected heartbeats for the three different configurations investigated. Visual inspection shows that both chest and head-shoulder recordings show recognizable QRS complexes. In contrast, the recording performed on auricular area does not show recognizable QRS complexes. This makes difficult to detect the heartbeat and thus the estimation of the heart rate (HR). Indeed, Bland-Altman analysis of HR estimated from head-shoulder ECG and ear-ECG respect to chest ECG demonstrates that head-shoulder derivation provides a far better HR estimation of the HR (using chest ECG as gold-standard) than that obtained from the auricular area (see Fig. 8 for Bland-Altman plot of a representative subject).

On contrast, HR values derived from PPG signals both, from finger and auricular provide good estimates of the HR. Fig. 9 shows an example of a combined chest-ECG and in-ear PPG recording together with Bland-Altman plots that demonstrate that the estimation of the HR from the PPG obtained in both regions is comparable to that obtained from the chest ECG.

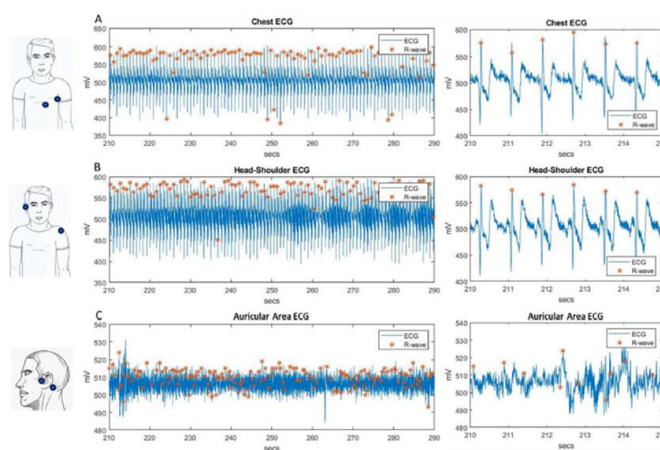


Fig. 7. Raw ECG measured on: A) the chest; B) between the ear and the contralateral shoulder; C) the auricular area. The body sketches on the left represent the location of the electrodes; the plots on the center 80s sample recorded on each area; and the plots on the right a 5s sample of the same signals.

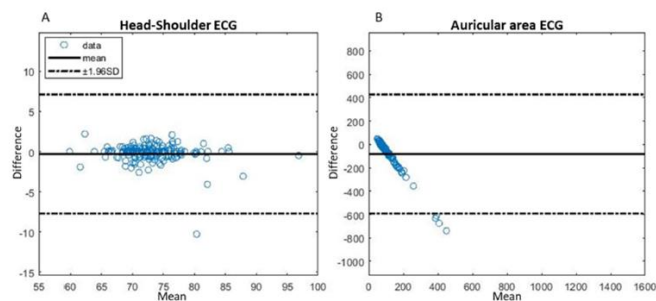


Fig. 8. Bland-Altman representation of the HR obtained from ECG from A) chest and head-shoulder, and B) chest and auricular area. Please, note the difference of scales in the two panels, as panel A) scales are [-15, 15] and [55, 100] bpm and for panel B) are [-1000, 900] and [0, 1600] bpm.

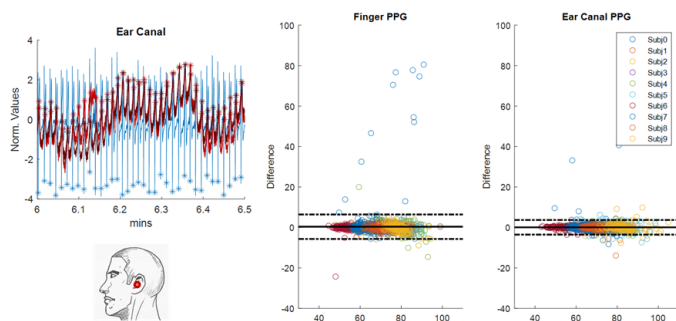


Fig. 9. Bland-Altman analysis for all subjects comparing the HR estimation on chest ECG against the finger PPG and auricular area PPG.

Fig. 10 shows an example of the capability of the MAX30102 PPG sensor to provide PPG information and SpO_2 information from the finger and three different points of the periauricular area. For the SpO_2 data, it should be noted 1) that these are non-calibrated estimates that serve to prove the feasibility of the measurements and 2) that the dimensions of the PCB hosting the PPG sensor difficulties the skin-sensor contact and this causes at some points movement-related artifacts in the SpO_2 estimation.

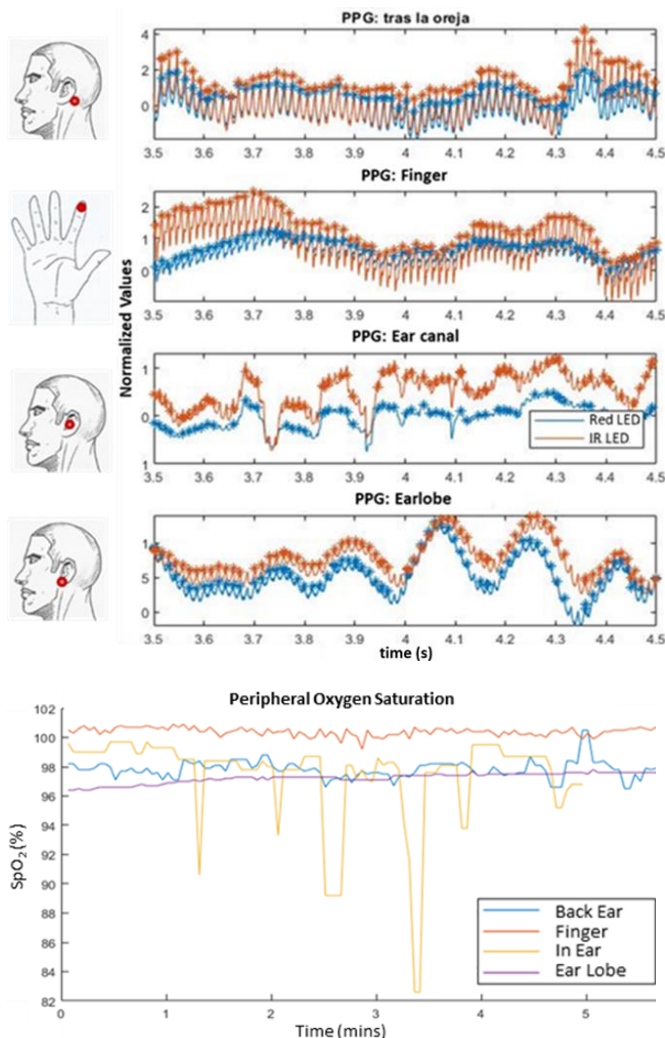


Fig. 10. PPG recordings on all four defined areas where blue plot represents red LED PPG and orange IR LED PPEG. The dots over each line represent the estimated location of a heartbeat. The exact placement of the sensor is indicated on the picture at the left of each graphic. SpO₂ estimated from PPG registers on the corresponding PPG recordings. The different levels of each area are due to non-calibrated estimation, and the severe artefacts on in ear registers are the results of an incompatible form factor of the sensor with ear canal.

D. Body Temperature

The comparative analysis of the three temperature sensors showed that the performance of the thermistor integrated in the MAX30102 PPG sensor was the lowest in terms of precision and dynamics of the response to temperature changes. On the other hand, and despite of the good performance of the MLX90615 IR temperature, this sensor was not considered as it fully blocks the ear canal, thus precluding the aeration and limiting the sound perception. As a result, we selected the TMP112 to proceed with the validation study on the 10 volunteers. As shown in Fig. 11 the effect on the temperature measured in the ear canal are barely affected by the changes in the room temperature. In contrast, the ambient sensor shows the effects of moving from room office to cold rooms at -5°C and -15°C and back to the office. All these results demonstrate the suitability of measuring the core temperature in the era canal as opposed to the use of wrist

worn sensors.

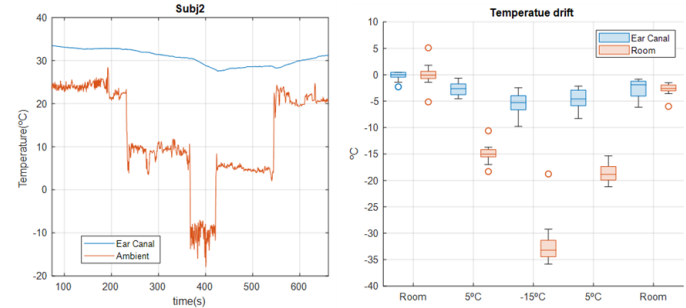


Fig. 11. A) Example of a representative volunteer of the temperature readings during the temperature validation study with the TMP112 measuring the ear canal temperature (blue) and a TMP102 measuring ambient temperature (orange). A) Temperature drift study for ear canal (blue) and ambient (orange) temperature through the different stages of the study. C) Table summarizing the mean and SD of the drifts for each ambient temperature the volunteers are exposed to.

E. Galvanic Skin Response

The GSR recordings on Fig. 12 illustrate the impossibility of the selected hardware to capture the modulation of the GSR in the periauricular region. Although it is capable to obtain significant (and similar) GSR modulations in both hands, no apparent modulation is observed when placing the electrodes between the tragus and the mastoid. Further statistical analysis on the four selected frequency bands ([0.1-0.2], [0.2-0.3], [0.3-0.4] and [0.4-1.0] Hz) confirms this observation, both for the Valsalva and video watching conditions (see Fig. 13).

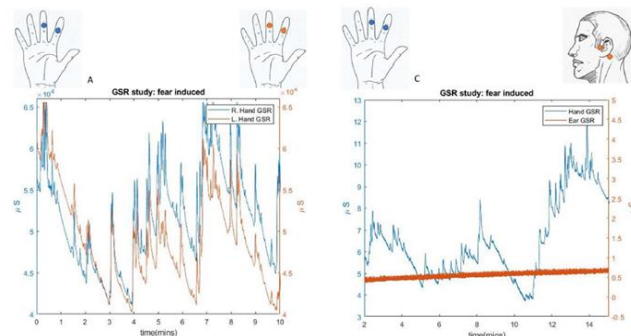


Fig. 12. Two examples of simultaneous GSR register on hand and auricular area represented in orange and blue respectively with independent axis associated by color. These are continuous recording going through the different Valsalva maneuvers.

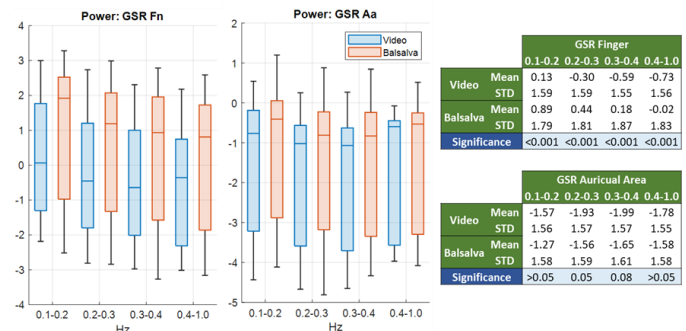


Fig. 13. Study of the power of the signal on the selected four frequency bands. The boxplots represent the power at the frequencies for the stimulation with the video (blue) and the Valsalva maneuver (orange): on the hand in the left and the auricular area on the left.

F. Proof of Concept Prototype

The results presented above did not only serve the purpose of validating the area for these measurements, but also to determine the suitability of the discrete electronic components selected. At this point, we then proceeded with the design and implementation of a "proof-of-concept" prototype aimed at determining the feasibility of a simultaneous recording of the selected measures through a unique microcontroller.

Fig. 14 shows this first prototype integrating 1) TMP112 thermistor for in-ear temperature measurement, 2) TMP102 for ambient temperature measurement, 3) MLX90615 IR thermometer for contactless tympanic temperature measurement, 4) MAX30102 for PPG recordings and 5) ADXL345 for acceleration recording. Schematics show the placement of the different components. Both TMP102 and ADXL345 are not placed directly on the periauricular area as the TMP102 is used to measure ambient temperature (thus, it is placed far from the area of recording) and the placement of the accelerometer does not require to be exactly the periauricular area but some convenient location on the head. All sensors include evaluation boards compatible with Arduino microcontrollers, except the TMP112. Therefore, a custom solution was generated to be compatible with this initial prototype and periauricular measurements. All sensors were controlled with an Arduino Nano that included a Bluetooth 4.0 transceiver to wirelessly broadcast the signals. Power supply was implemented by means of a 3.7V lithium-ion battery and a TTL port for manual event input or synchronization purposes was included. All mentioned components were attached (with Velcro or screws) to a head harness with an adjustable fastening system to fit with the different head sizes.

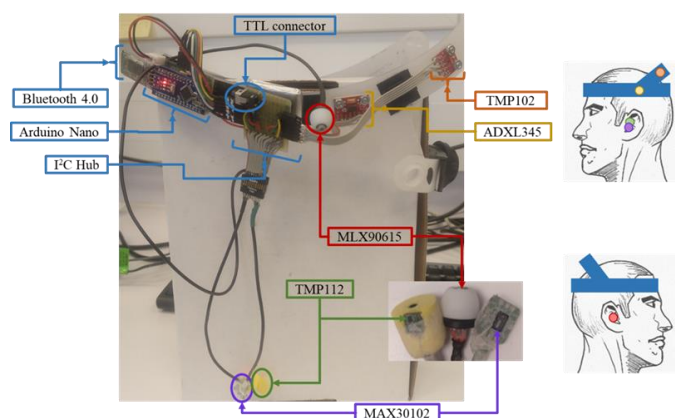


Fig. 14. Proof of concept prototype build around head harness including the following sensors: TMP102 (orange), TMP112 (green), ADXL345 (yellow), MAX30102 (purple) and MLX90615 (red). In blue indicated the remaining components for management, connection and computing: Arduino Nano, lithium battery, Bluetooth 4.0, TTL connector and I2C hub. The head sketches presented represent the placement of each component according to their color code.

Finally, the set up was completed with the addition of an EEG signal recorded through a *BrainVision* system with electrodes places in the periauricular area (see above). In the current version of the prototype EEG data was not directly recorded by the Arduino Nano but synchronized with the

BrainVision system by using of the TTL port included. Thus, the set up demonstrates the feasibility of implementing the acquisition of the EEG, PPG and core temperature from the periauricular area, together with accelerometry and room temperature signals simultaneously. Fig. 15 shows an example of one recording during a α -band modulation study. The EEG data coming from the EarSup electrode shows a clear modulation of the α rhythm when subject was asked to close his eyes and press the TTL marker. This marker was recorded in the presented in the *BrainVision* system this picture has been filtered with a band-pass filter between 0.5 and 35 Hz, removing the high frequency and line noise and accentuating the α -band modulation on the EarSup electrode. The TTL channel shows the states of the volunteer: open (blue) and close (green) eyes. As can be seen, there is an increment on the activity of the EEG recording during the closed-eyes period, corresponding to ~ 10 Hz. The remaining parameters are correctly recorded: a) the temperature shows the expected stable parameters; b) the red and IR PPG signals show the waveform corresponding to each heartbeat synchronized for both signals; c) the acceleration shows stable acceleration measurements, despite some alterations due to subjects' movements to accommodate on the chair.

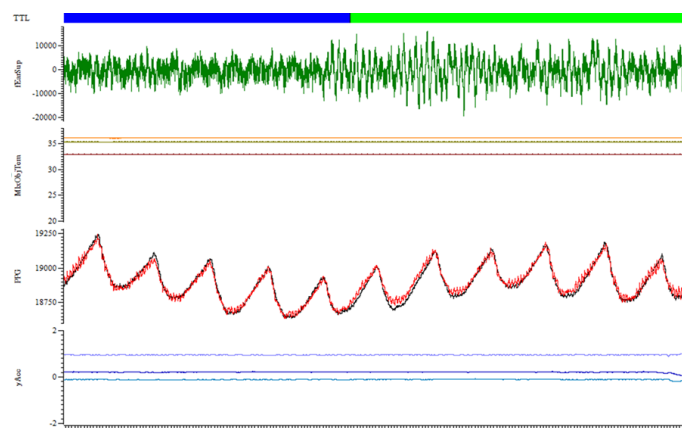


Fig. 15. Sample of the recordings obtained with the presented proof of concept prototype and the *BrainVision* showing the four signal modalities and the TTL registers combined on a single recording.

G. Body Area Network Wireless Connectivity

In order to gain insight in relation with the feasibility of employing BAN transceivers within the multimodal signal platform, coverage/capacity estimations have been obtained for Bluetooth Classic as well as for Bluetooth Low Energy (BLE). Different body area network topologies have been considered, following the path loss methodology described in [64], which considers receiver position at chest or hip and transmitter positions at chest, back, right wrist and left wrist. The maximum data transmit power has been fixed to 10 dBm for both types of transceivers, considering that adaptive frequency hopping (AFH) is not active or that there are less than 15 channels available (in order to consider a more restrictive use case scenario; if AFH is active, then 20 dBm maximum transmission power is feasible). Receiver sensitivity thresholds have been set to -70 dBm for Bluetooth Classic and BLE 1M/2M, whereas for the case of BLE coded ($s=2$) it has

been set to -78 dBm and for BLE coded ($s=8$) to -85 dBm, following core Bluetooth specifications. The results are presented in Fig. 16 and as it can be seen, received power levels are in principle above sensitivity thresholds for all the link types under consideration. Further tests however are compulsory in order to evaluate wireless channel performance as a function of noise floor variations (owing to variable interference conditions and considering different interference sources, i.e., intra-system, inter-system and external sources) and site-specific propagation conditions.

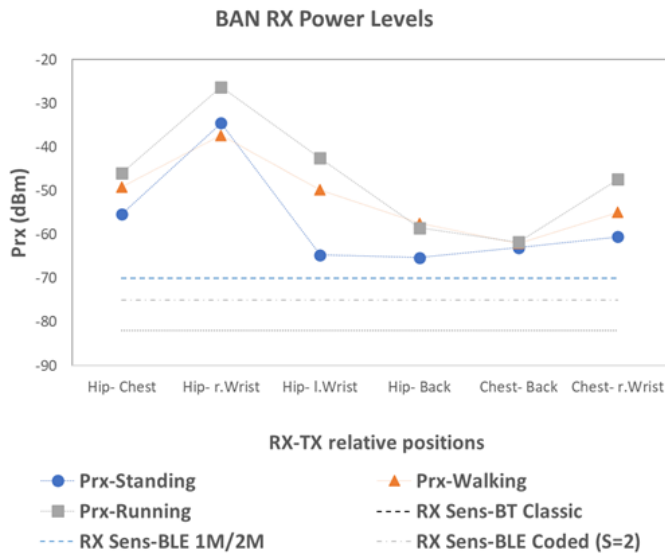


Fig. 16. Estimation of received power levels in relation with relative TX-RX positions within a body area network configuration. The values consider the use of Bluetooth as well as Bluetooth Low Energy transceivers.

In order to assess the behavior of inter/intra-body wireless links with the operating range of BT/BLE systems (center operating frequency of 2.4 GHz), deterministic full wave simulations have been performed with the aid of CST Microwave Studio. The human body voxel model ‘Gustav’ has been employed, providing accurate frequency dispersive material characteristics. The CST Voxel Family is composed of different human body models, from eight persons of different gender, age and stature. The biological data of all tissues present in human bodies are considered, as well as their electric properties such as permittivity and conductivity [65]. In Fig. 17 the ‘Gustav’ voxel model employed for the simulations described in this work can be seen. The numbered points represent the proposed location of the antennas for the wireless link analysis (the green dot represents the transmitter, emulating our sensor device, and the red ones the receivers). It is worth noting that, in this case, transceiver location is flexible and hence, can be located in a more convenient location (e.g., transmitter in the periauricular area), as compared to previous wireless link model employed.

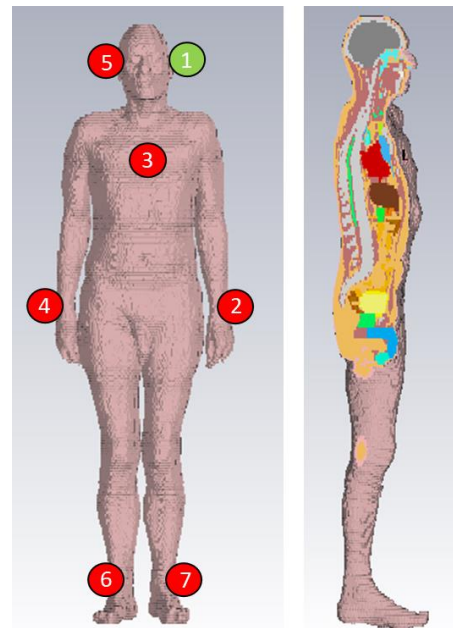
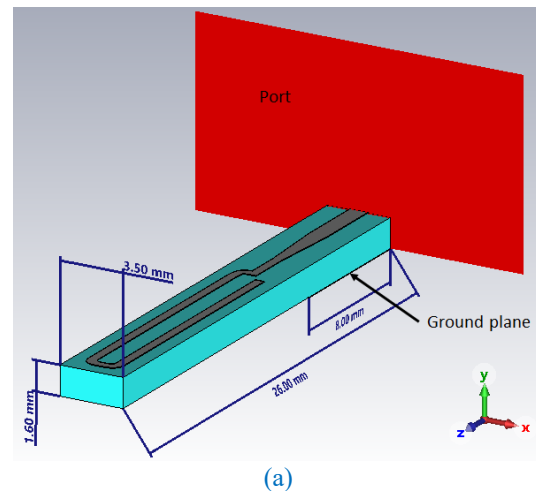


Fig. 17. The human body model employed for body area wireless link simulations. The numbered green dot represents the transmitter location, and the red dots the receiver locations.

An antenna has been designed for the CST Microwave simulation, following the criteria of operating at 2.4 GHz and being as small as possible. Note that this antenna has been designed simplified for the wireless link analysis, and the antenna integrated in the sensor device will be different after considering the encapsulation of the whole device. Fig. 18 shows the designed antenna. The substrate is FR4 (dielectric constant = 4.37) and metallic parts are copper.



(a)

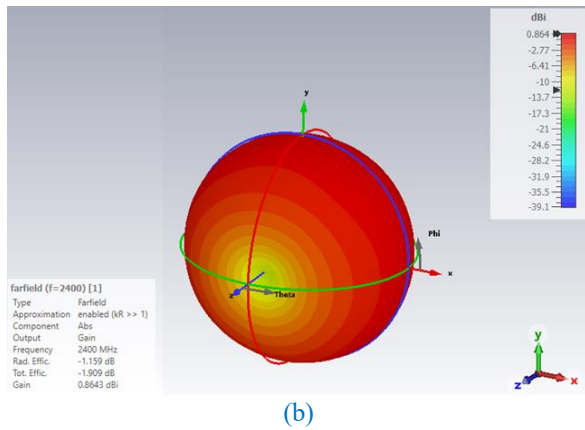


Fig. 18. (a) Antenna designed for the CST simulations (b) Radiation pattern of the antenna.

This antenna has been included as transmitter and receiver at different points on the human body model in the simulation scenario presented in Fig. 17. Specifically, the transmitter has been located at the left ear, and the receivers at the right ear, on the chest, both wrists and both ankles. Fig. 19 presents the electric field distribution obtained by the CST Microwave Studio simulations. The employed human body allows obtaining propagation estimations in the air, in the body and on the body.

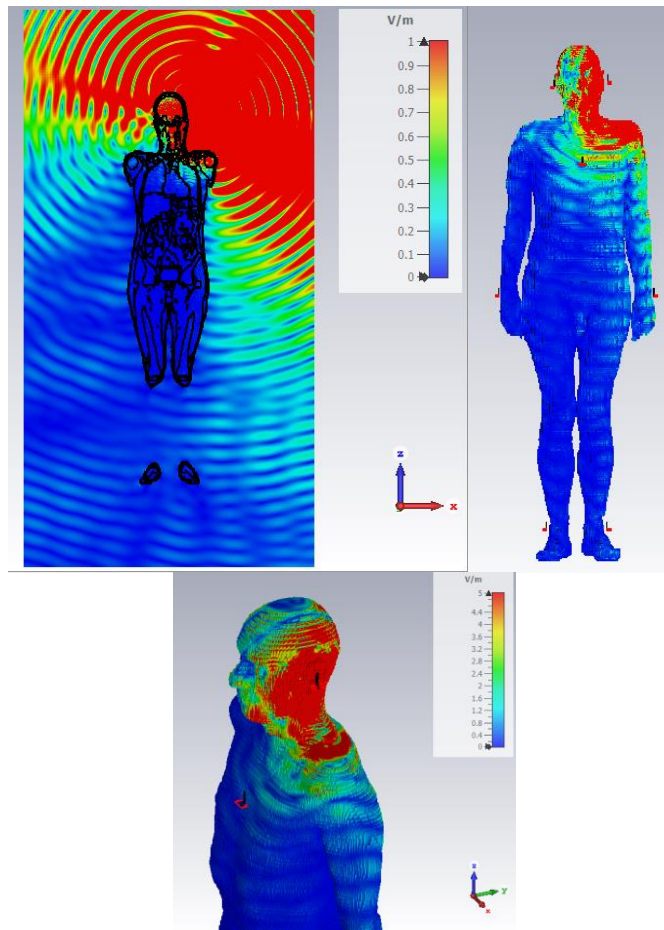


Fig. 19. CST Microwave Studio results: Electric field distribution (both through the air, in and on the human body) generated by the transmitter, located at the left ear.

The electric field propagation results and the inclusion of the antennas at the mentioned locations lead to the analysis of the wireless link in terms of the S_{21} parameter (i.e. transmission parameter), which represents the energy from the transmitter received by each receiver antenna (from the transmitter). The values of received power levels obtained for each one of the transceiver locations is given in Table I. The results show that received power levels in this case are lower, which is given on one hand in the difference in relation with the relative position of the transmitter-receiver pairs and on the other hand, on a more precise consideration of human body impact as well as on the performance degradation of the realistic antenna model employed.

TABLE I
RECEIVER POWER LEVELS-FULL WAVE RESULTS

Receiver Location (TX in Left Ear)	RX Power Level (dBm)
Left wrist	-69,53
Chest	-64,48
Right wrist	-97,93
Right ear	-91,16
Right ankle	-103,75
Left ankle	-81,64

IV. CONCLUSION

The measurement of the purposed parameters has been fulfilled with mixed results. On one hand, the selected setup on the auricular area for PPG, acceleration temperature and EEG show an adequate behavior for the application purposed.

The ADX345 is capable of recording distinctive acceleration patterns corresponding to each activity tested, enabling the quantification of their similarities, and allowing future applications of motion classification. All temperature sensors provide adequate response to the different testing, being the TMP112 thermistor the selected sensor for both integration and validation studies given its behavior, robustness and reduced dimensions. The drop-in temperature of 5.4°C measured during the very cold environment exposure (where the user is exposed to 31.8°C drop) shows that the area has the potential to provide adequate temperature measurements once the sensor placement and isolation are better approached. Nevertheless, this deviation of the measurements can be easily avoided by the use of protective clothing. In terms of PPG, the performed test showed that the behavior of this measurement on the auricular area is equivalent to its measurement on the gold standard on the finger. The HR and PTT studies showed the adequacy of the auricular area to acquire this signal modality. Moreover, the MAX30102 sensor can record the signal in the area of interest with enough quality to assess properly SpO2 and HR related parameters. In case of EEG, the results show that it is possible to detect the α -modulation during an opened/closed eyes test as well as VEP and VSSR's. However, the equipment used does not admit integration with the rest of devices, thus a discrete device capable of similar (or better) recordings has to be selected.

On contrast to these four parameters, both ECG and GSR are discarded. Even with the restrictive electrode configuration, auricular area ECG records some cardiac activity with very low amplitude and inconsistent presence among subjects. However,

as mentioned before the PPG recordings show high signal quality and temporal coherence with the ECG being a great substitute for temporal characterization. In a similar manner, the GSR requires skin areas with enough separation between them to create some resistance to the applied current and active enough sweat glands during sympathetic arousal. Fortunately, multiple studies show that, despite being related to different physiological phenomena, both HRV and GSR can be used to assess the same type of emotional and sympathetic arousal. So, with the appropriate analysis tools GSR can be substituted by the PPG. Nevertheless, GSR and ECG quality issues might be overcome with hardware modification, searching more adequate hardware or customized devices.

For the validation of four of the parameters, a wearable device has been developed integrating multiple temperature sensors, acceleration and PPG devices. The current state of this prototype lacks a proper EEG integration to be considered complete. Despite this limitation solved by synchronization through the TTL port, the volunteers wearing this system reported minor inconvenience in its use and sensors placement on the auricular area. This and the quality of the recording, further validates the implementation and serves as a basis for future more ambitious implementations miniaturizing this device and upgrading its functionalities.

Even with the restrictiveness of the selected area for physiological signal recording, here we have shown that it is feasible to obtain physiological data from the selected region. By doing so, we consider that it is possible to implement a wearable solution to determine the subject's state in an ergonomic and reliable way. In addition, Body Area Network Wireless Connectivity analyses demonstrate the feasibility and limitations in terms of coverage/capacity conditions, as well as detailed impact of human body presence intra/inter body links.

A device built for this purpose would not only be of great aid for epileptic patients and their relatives, it will also be capable of detecting fever, motility disturbances and low oxygen saturation; all of them very convenient for COVID-19 monitoring and early detection. Future work is also foreseen in the integration of wireless communication capabilities with BAN protocols as well as exploring further alternatives such as Low Power Wide Area Network protocols, 5G NR FR1 (below 6 GHz bands, machine type communications) or IEEE 802.11ah (sub 1 GHz IoT purpose specific connectivity).

REFERENCES

- [1] M. W. J. Huygens et al., "Self-monitoring of health data by patients with a chronic disease: does disease controllability matter?," *BMC Fam. Pract.*, vol. 18, no. 1, p. 40, Mar. 2017.
- [2] M. W. J. Huygens, J. Vermeulen, I. C. S. Swinkels, R. D. Friele, O. C. P. van Schayck, and L. P. de Witte, "Expectations and needs of patients with a chronic disease toward self-management and eHealth for self-management purposes," *BMC Health Serv. Res.*, vol. 16, no. 1, p. 232, Dec. 2016.
- [3] R. V. Milani, R. M. Bober, and C. J. Lavie, "The Role of Technology in Chronic Disease Care," *Progress in Cardiovascular Diseases*, vol. 58, no. 6, W.B. Saunders, pp. 579–583, May-2016.
- [4] D. V. Gunasekeran, "Technology and chronic disease management.," *lancet. Diabetes Endocrinol.*, vol. 6, no. 2, p. 91, Feb. 2018.
- [5] K. Lancaster et al., "The Use and Effects of Electronic Health Tools for Patient Self-Monitoring and Reporting of Outcomes Following Medication Use: Systematic Review," *J Med Internet Res* 2018;20(12)e294 <https://www.jmir.org/2018/12/e294>, vol. 20, no. 12, p. e294, Dec. 2018.
- [6] J. M. Peake, G. Kerr, and J. P. Sullivan, "A Critical Review of Consumer Wearables, Mobile Applications, and Equipment for Providing Biofeedback, Monitoring Stress, and Sleep in Physically Active Populations.," *Front. Physiol.*, vol. 9, p. 743, 2018.
- [7] M. Zhang, M. Luo, R. Nie, and Y. Zhang, "Technical attributes, health attribute, consumer attributes and their roles in adoption intention of healthcare wearable technology," *Int. J. Med. Inform.*, vol. 108, pp. 97–109, Dec. 2017.
- [8] J. M. Tsai, M. J. Cheng, H. H. Tsai, S. W. Hung, and Y. L. Chen, "Acceptance and resistance of telehealth: The perspective of dual-factor concepts in technology adoption," *Int. J. Inf. Manage.*, vol. 49, pp. 34–44, Dec. 2019.
- [9] M. S. Rahman, "Does Privacy Matters When We are Sick? An Extended Privacy Calculus Model for Healthcare Technology Adoption Behavior," 2019 10th Int. Conf. Inf. Commun. Syst. ICICS 2019, pp. 41–46, Jun. 2019.
- [10] L. Hogaboam and T. Daim, "Technology adoption potential of medical devices: The case of wearable sensor products for pervasive care in neurosurgery and orthopedics," *Heal. Policy Technol.*, vol. 7, no. 4, pp. 409–419, Dec. 2018.
- [11] E. Bruno, P. F. Viana, M. R. Sperling, and M. P. Richardson, "Seizure detection at home: Do devices on the market match the needs of people living with epilepsy and their caregivers?," *Epilepsia*, vol. 61, no. S1, pp. S11–S24, Nov. 2020.
- [12] T. Rukasha, S. I. Woolley, T. Kyriacou, and T. Collins, "Evaluation of Wearable Electronics for Epilepsy: A Systematic Review," *Electron. 2020*, Vol. 9, Page 968, vol. 9, no. 6, p. 968, Jun. 2020.
- [13] C. E. Stafstrom and L. Carmant, "Seizures and Epilepsy: An Overview for Neuroscientists," *Cold Spring Harb. Perspect. Med.*, vol. 5, no. 6, p. a022426, Jun. 2015.
- [14] O. Devinsky et al., "Epilepsy," *Nat. Rev. Dis. Prim.* 2018 41, vol. 4, no. 1, pp. 1–24, May 2018.
- [15] L. Lagae, J. Irwin, E. Gibson, and A. Battersby, "Caregiver impact and health service use in high and low severity Dravet syndrome: A multinational cohort study.," *Seizure*, vol. 65, pp. 72–79, Feb. 2019.
- [16] J. Pimentel, "The epileptic multifactorial patient's burden. Review of the topic," *J. Epileptol.*, vol. 24, no. 2, pp. 167–172, Sep. 2016.
- [17] G. H. Kim, J. H. Byeon, S. H. Eun, and B. L. Eun, "Parents' Subjective Assessment of Effects of Antiepileptic Drug Discontinuation," *J. Epilepsy Res.*, vol. 5, no. 1, pp. 9–12, Jun. 2015.
- [18] M. Teplan, "Fundamentals of EEG Measurement," *Meas. Sci. Rev.*, vol. 2, no. 2, 2002.
- [19] S. Noachtar and J. Rémi, "The role of EEG in epilepsy: A critical review," *Epilepsy and Behavior*, vol. 15, no. 1. Academic Press, pp. 22–33, May-2009.
- [20] K. B. Mikkelsen, S. L. Kappel, D. P. Mandic, and P. Kidmose, "EEG recorded from the ear: Characterizing the Ear-EEG Method," *Front. Neurosci.*, vol. 9, no. NOV, pp. 1–8, 2015.
- [21] A. Paul, S. R. Deiss, D. Tourtelotte, M. Kleffner, T. Zhang, and G. Cauwenberghs, "Electrode-Skin Impedance Characterization of In-Ear Electrophysiology Accounting for Cerumen and Electrodermal Response," in *International IEEE/EMBS Conference on Neural Engineering, NER, 2019*, vol. 2019-March, pp. 855–858.
- [22] M. Eickenscheidt, P. Schäfer, Y. Baslan, C. Schwarz, and T. Stieglitz, "Highly porous platinum electrodes for dry ear-EEG measurements," *Sensors (Switzerland)*, vol. 20, no. 11, pp. 1–12, Jun. 2020.
- [23] C. Athavipach, S. Pan-Ngum, and P. Israsena, "A wearable in-ear EEG device for emotion monitoring," *Sensors (Switzerland)*, vol. 19, no. 18, p. 4014, Sep. 2019.
- [24] V. Goverdovsky et al., "Hearables: Multimodal physiological in-ear sensing," *Sci. Rep.*, vol. 7, no. 1, pp. 1–10, 2017.
- [25] M. G. Bleichner and S. Debener, "Concealed, Unobtrusive Ear-Centered EEG Acquisition: cEEGrids for Transparent EEG.," *Front. Hum. Neurosci.*, vol. 11, p. 163, Apr. 2017.
- [26] Y. Gu et al., "Comparison between scalp EEG and behind-the-ear EEG for development of a wearable seizure detection system for patients with focal epilepsy," *Sensors (Switzerland)*, vol. 18, no. 1, p. 29, Jan. 2018.
- [27] I. C. Zibrandtsen, P. Kidmose, C. B. Christensen, and T. W. Kjaer, "Ear-EEG detects ictal and interictal abnormalities in focal and generalized epilepsy – A comparison with scalp EEG monitoring," *Clin. Neurophysiol.*, vol. 128, no. 12, pp. 2454–2461, 2017.

- [28] S. M. Rissanen et al., "Wearable monitoring of positive and negative myoclonus in progressive myoclonic epilepsy type 1," *Clin. Neurophysiol.*, vol. 132, no. 10, pp. 2464–2472, Oct. 2021.
- [29] D. Castaneda, A. Esperanze, M. Ghamari, C. Soltanpur, and H. Nazeran, "A review on wearable photoplethysmography sensors and their potential future applications in health care," *Int. J. Biosens. Bioelectron.*, vol. 4, no. 4, pp. 195–202, 2018.
- [30] G. J. Horng and K. H. Chen, "The Smart Fall Detection Mechanism for Healthcare Under Free-Living Conditions," *Wirel. Pers. Commun.* 2021 1181, vol. 118, no. 1, pp. 715–753, Jan. 2021.
- [31] J. P. Wolff, F. Grützmaier, A. Wellnitz, and C. Haubelt, "Activity recognition using head worn inertial sensors," in *ACM International Conference Proceeding Series*, 2018, pp. 1–7.
- [32] M. AlGhatrif and J. Lindsay, "A brief review: history to understand fundamentals of electrocardiography," <http://dx.doi.org/10.3402/jchimp.v2i1.14383>, vol. 2, no. 1, p. 14383, Jan. 2012.
- [33] K. Khunti, "Accurate interpretation of the 12-lead ECG electrode placement: A systematic review," *Health Educ. J.*, vol. 73, no. 5, pp. 610–623, 2014.
- [34] L. Billeci, A. Tonacci, D. Marino, L. Insana, G. Vatti, and M. Varanini, "A Machine Learning Approach for Epileptic Seizure Prediction and Early Intervention," in *Biosystems and Biorobotics*, vol. 21, Springer International Publishing, 2019, pp. 972–976.
- [35] A. van Westrhenen, T. De Cooman, R. H. C. Lazeron, S. Van Huffel, and R. D. Thijs, "Ictal autonomic changes as a tool for seizure detection: a systematic review," *Clinical Autonomic Research*, vol. 29, no. 2. Dr. Dietrich Steinkopff Verlag GmbH and Co. KG, pp. 161–181, Apr-2019.
- [36] G. Giannakakis, M. Tsiknakis, and P. Vorgia, "Focal epileptic seizures anticipation based on patterns of heart rate variability parameters," *Comput. Methods Programs Biomed.*, vol. 178, pp. 123–133, Sep. 2019.
- [37] Y. Sun and N. Thakor, "No TitlePhotoplethysmography Revisited: From Contact to Noncontact, From Point to Imaging," *IEEE Trans. Biomed. Eng.*, vol. 63, no. 3, pp. 463–477, 2016.
- [38] J. Allen, "Photoplethysmography and its application in clinical physiological measurement," *Physiol. Meas.*, vol. 28, no. 3, pp. R1–R39, Mar. 2007.
- [39] Y. Maeda, M. Sekine, and T. Tamura, "Relationship Between Measurement Site and Motion Artifacts in Wearable Reflected Photoplethysmography," *J. Med. Syst.* 2010 355, vol. 35, no. 5, pp. 969–976, May 2010.
- [40] S. Bagha, S. Hills, P. Bhubaneswar, and L. Shaw, "A Real Time Analysis of PPG Signal for Measurement of SpO₂ and Pulse Rate," *Int. J. Comput. Appl.*, vol. 36, no. 11, pp. 975–8887, 2011.
- [41] R. J. Thomas, J. E. Mietus, C. K. Peng, and A. L. Goldberger, "An electrocardiogram-based technique to assess cardiopulmonary coupling during sleep," *Sleep*, vol. 28, no. 9, pp. 1151–1161, Sep. 2005.
- [42] C. Varon, K. Jansen, L. Lagae, L. Faes, and S. Van Huffel, "Transient behavior of cardiorespiratory interactions towards the onset of epileptic seizures," *Comput. Cardiol.* (2010), vol. 41, pp. 917–920, 2014.
- [43] C. Varon et al., "Interictal cardiorespiratory variability in temporal lobe and absence epilepsy in childhood," *Physiol. Meas.*, vol. 36, no. 4, pp. 845–856, Apr. 2015.
- [44] S. Passler, N. Müller, and V. Senner, "In-Ear Pulse Rate Measurement: A Valid Alternative to Heart Rate Derived from Electrocardiography?," *Sensors* 2019, Vol. 19, Page 3641, vol. 19, no. 17, p. 3641, Aug. 2019.
- [45] V. Bach, F. Telliez, and J. P. Libert, "The interaction between sleep and thermoregulation in adults and neonates," *Sleep Med. Rev.*, vol. 6, no. 6, pp. 481–92, Dec. 2002.
- [46] A. K. C. Leung, K. L. Hon, and T. N. H. Leung, "Febrile seizures: an overview," *Drugs Context*, vol. 7, 2018.
- [47] M. Sund-Levander, C. Forsberg, and L. K. Wahren, "Normal oral, rectal, tympanic and axillary body temperature in adult men and women: A systematic literature review," *Scand. J. Caring Sci.*, vol. 16, no. 2, pp. 122–128, Jun. 2002.
- [48] R. Norman, L. Mendolicchio, and C. Mordeniz, "Galvanic Skin Response & Its Neurological Correlates," *J. Conscious. Explor. Res.*, vol. 7, no. 7, pp. 553–572, 2016.
- [49] R. L. Bailey, "Electrodermal Activity (EDA)," *Int. Encycl. Commun. Res. Methods*, pp. 1–15, 2017.
- [50] R. Martinez, A. Salazar-Ramirez, A. Arruti, E. Irigoyen, J. I. Martin, and J. Muguerza, "A Self-Paced Relaxation Response Detection System Based on Galvanic Skin Response Analysis," *IEEE Access*, vol. 7, pp. 43730–43741, 2019.
- [51] M.-Z. Poh et al., "Convulsive seizure detection using a wrist-worn electrodermal activity and accelerometry biosensor," *Epilepsia*, vol. 53, no. 5, pp. e93–e97, May 2012.
- [52] R. W. Picard et al., "Wrist sensor reveals sympathetic hyperactivity and hypoventilation before probable SUDEP," *Neurology*, vol. 89, no. 6, pp. 633–635, Aug. 2017.
- [53] M. van Dooren, J. J. G. G. J. de Vries, and J. H. Janssen, "Emotional sweating across the body: Comparing 16 different skin conductance measurement locations," *Physiol. Behav.*, vol. 106, no. 2, pp. 298–304, May 2012.
- [54] C. J. Smith and G. Havenith, "Body mapping of sweating patterns in male athletes in mild exercise-induced hyperthermia," *Eur. J. Appl. Physiol.*, vol. 111, no. 7, pp. 1391–1404, Jul. 2011.
- [55] S. L. Kappel, M. L. Rank, H. O. Toft, M. Andersen, and P. Kidmose, "Dry-Contact Electrode Ear-EEG," *IEEE Trans. Biomed. Eng.*, vol. 66, no. 1, pp. 150–158, Jan. 2019.
- [56] P. Stoica and R. Moses, *Spectral Analysis Of Signals*. 2005.
- [57] B. Porat, *Digital Processing of Random Signals: Theory and Methods*. 2008.
- [58] D. J. Creel, "Visually evoked potentials," *Handb. Clin. Neurol.*, vol. 160, pp. 501–522, Jan. 2019.
- [59] M. Müller, "Dynamic Time Warping," *Inf. Retr. Music Motion*, pp. 69–84, 2007.
- [60] R. Musculo, S. Conforto, M. Schmid, P. Caselli, and T. D'Alessio, "Classification of motor activities through derivative dynamic time warping applied on accelerometer data," *Annu. Int. Conf. IEEE Eng. Med. Biol. - Proc.*, pp. 4930–4933, 2007.
- [61] N. Ö. Doğan, "Bland-Altman analysis: A paradigm to understand correlation and agreement," *Turkish J. Emerg. Med.*, vol. 18, no. 4, pp. 139–141, Dec. 2018.
- [62] R. Zangróniz, A. Martínez-Rodrigo, J. M. Pastor, M. T. López, and A. Fernández-Caballero, "Electrodermal activity sensor for classification of calm/distress condition," *Sensors (Switzerland)*, vol. 17, no. 10, pp. 1–14, 2017.
- [63] D. B. Smith, D. Miniutti, T. A. Lamahewa and L. W. Hanlen, "Propagation Models for Body-Area Networks: A Survey and New Outlook," in *IEEE Antennas and Propagation Magazine*, vol. 55, no. 5, pp. 97–117, Oct. 2013.
- [64] D. Smith, D. Miniutti, L. Hanlen, A. Zhang, D. Lewis, D. Rodda, et al., "Power Delay Profiles for Dynamic Narrowband Body Area Network Channels ID:802.15-09-0187-01-0006," *IEEE submission*, March 2009.
- [65] CST Human Body model, https://space.mit.edu/RADIO/CST_online/mergedProjects/3D/common_tools/common_tools_biomodels.htm